COMMUNICATIONS: SIF Congress 2017

$\psi(2S)$ production in p-Pb collisions at $\sqrt{s_{\mathrm{NN}}} = 8.16$ TeV

L. MICHELETTI(*)

INFN, Sezione di Torino - Torino, Italy

Summary. — The inclusive production of the charmonium state $\psi(2S)$ was studied at $\sqrt{s_{\mathrm{NN}}} = 8.16$ TeV in proton-lead collisions, using the ALICE detector at the CERN LHC. The measurement is performed in the two centre of mass rapidity ranges, $2.03 < y_{\mathrm{cms}} < 3.53$ and $-4.46 < y_{\mathrm{cms}} < -2.96$, by reconstructing the $\psi(2S)$ decay to a muon pair. The results are compared to those obtained for the J/ψ at the same centre of mass energy by showing the ratios between the J/ψ and $\psi(2S)$ production cross sections and by studying the nuclear modification factor (R_{pA}) as a function of transverse momentum $(p_{\mathrm{T}} < 12\,\mathrm{GeV}/c)$ and rapidity. The comparison with $\psi(2S)$ results in proton-lead collisions at $\sqrt{s_{\mathrm{NN}}} = 5.02$ TeV and theoretical predictions is also shown.

1. – Introduction

The study of charmonia, bound states of a charm and anti-charm quarks $(c\bar{c})$, represents a research field of particular interest in the investigation of Quark Gluon Plasma (QGP) properties. In fact the production of these mesons is expected to be modified when a strongly interacting deconfined medium is produced, by means of a screening mechanism due to the high density of colour charges [1]. This leads to a suppression of the yields of charmonia in nucleus-nucleus collisions with respect to the proton-proton ones. At LHC energies $c\bar{c}$ pairs are produced in large number, hence charmonium suppression can be partly counterbalanced by a "regeneration" mechanism, which is related to the charmonium formation through the statistical recombination of charm quarks. These effects can be quantified through the evaluation of the nuclear modification factor (R_{AA}), defined as the ratio between the A-A and pp charmonium production cross sections normalized to the number of nucleon-nucleon collisions.

In nucleus-nucleus collisions there are also effects which are not related to the formation of a deconfined medium, hence it becomes important to quantify these mechanisms

---

(*) E-mail: luca.micheletti@to.infn.it

and their influence on charmonium production. These effects are studied in proton-nucleus collisions, where no QGP formation is supposed to take place, and they are known as *cold nuclear matter effects*. One of them is the *nuclear shadowing* which consists in the modification of the quark and gluon structure functions for a nucleon inside nuclei. Another effect is the *coherent energy loss* which determines a modification of parton kinematics and it is related to the gluon radiation [2]. Finally charmonium can be dissociated interacting with colliding nuclei. This effect, named *nuclear absorption*, is relevant when the formation time of the resonance is smaller than the time spent by the $c\bar{c}$ inside the nucleus and it is not playing a role at LHC energies.

In this paper ALICE results on $\psi(2S)$ production at $\sqrt{s_{\mathrm{NN}}} = 8.16\,\mathrm{TeV}$ in proton-nucleus collisions are reported. Results are presented in terms of the nuclear modification factor as a function of p_{T} ($p_{\mathrm{T}} < 12\,\mathrm{GeV}/c$) and in two rapidity ranges ($2.03 < y_{\mathrm{cms}} < 3.53$ and $-4.46 < y_{\mathrm{cms}} < -2.96$) and they are compared with the R_{pA} of J/ψ at $\sqrt{s_{\mathrm{NN}}} = 8.16\,\mathrm{TeV}$ [3] and of $\psi(2S)$ at $\sqrt{s_{\mathrm{NN}}} = 5.02\,\mathrm{TeV}$ [4]. R_{pA} are then compared with theoretical predictions.

2. – Experimental apparatus, data sample and event selection

The ALICE detector design and performance are described in [5] and [6]. In this analysis the $\psi(2S)$ is studied in its muon pair decay, hence the Muon Spectrometer has a crucial role in this study. It is composed by a system of passive absorbers, a dipole magnet, a muon tracker, a passive iron wall and a muon trigger system. Other detectors involved in this analysis are the V0 scintillator hodoscopes, which are used for triggering purposes, and the Zero Degree Calorimeters (ZDC), mainly used for the centrality determination.

Data used for this analysis have been collected with two different beam configurations, obtained by inverting the direction of the orbits of two colliding beams. The ranges $2.03 < y_{\mathrm{cms}} < 3.53$ and $-4.46 < y_{\mathrm{cms}} < -2.96$ are accessible, where positive rapidities correspond to the situation in which the proton beam is going towards the Muon Spectrometer while negative ones refer to the situation in which the Pb beam is travelling towards the spectrometer. Data have been collected at the centre of mass energy of $8.16\,\mathrm{TeV}$, in November-December 2016. The data samples used in this analysis correspond to the integrated luminosity $L_{\mathrm{int}}^{\mathrm{pPb}} \sim 8.7\,\mathrm{nb}^{-1}$ for the p-Pb configuration and $L_{\mathrm{int}}^{\mathrm{pPb}} \sim 12.9\,\mathrm{nb}^{-1}$ for the Pb-p one.

Minimum-bias events are triggered requiring that the coincidence of a signal in the two V0 detectors and the efficiency of such a trigger is better than 99%. Opposite-sign muon pairs are selected by means of a dimuon trigger given by the coincidence of a MB trigger with the detection of two muon candidate tracks in the trigger system of the Muon Spectrometer. This trigger is configured in order to select muons with a transverse momentum $p_{\mathrm{T}} > 0.5\,\mathrm{GeV}/c$. An offline selection is performed in order to reject background due to beam interactions by requiring the signal timing in the V0 and ZDC to be compatible with that of a nominal p-Pb (Pb-p) interaction. Candidate muon tracks are reconstructed in the muon tracking chambers using the standard reconstruction algorithm [7], then requiring that:

- both muon tracks in the tracking chambers must match a track reconstructed in the trigger system;

- tracks are selected in the pseudo-rapidity range $-4 < \eta < -2.5$ in order to reject tracks at the edges of the detector's acceptance;

- the transverse radius of the track at the end of the front absorber is in the range $17.6 \leq R_{\mathrm{abs}} \leq 89.5$ cm, removing tracks passing through the thicker part of the front absorber;

- the dimuon rapidity is in the range $2.5 \leq y_{\mathrm{cms}} \leq 4$.

3. – Data analysis

The inclusive $\psi(2S)$ production cross section is computed as

$$(1) \qquad \sigma_{pA}^{\psi(2S)} = \frac{N_{\psi(2S)\to\mu^+\mu^-}}{L_{int}^{pA} \cdot (A \times \epsilon)_{\psi(2S)\to\mu^+\mu^-} \cdot B.R._{\cdot\psi(2S)\to\mu^+\mu^-}},$$

where $N_{\psi(2S)}$ is the number of $\psi(2S)$ produced in p-Pb and Pb-p collisions corrected by the acceptance $\times$ efficiency $(A \times \epsilon)$, L_{int} is the integrated luminosity and $B.R.$ is the branching ratio for the decay to a muon pair $B.R._{\cdot\psi(2S)\to\mu^+\mu^-} = (7.9 \pm 0.8) \times 10^{-3}$ [8]).

$N_{\psi(2S)}$ is obtained through a signal extraction procedure, which consists in fitting the opposite sign dimuon invariant mass distribution with different functions. In details the fitting functions are the sum of the contributions of the J/ψ and $\psi(2S)$ signals and background. For the signals the "extended" Crystal Ball (CB2) and the NA60 functions are used [9], both of them characterized by a Gaussian core and non-Gaussian tails. The tails parameters are fixed, in the fitting procedure, to the values extracted from the Monte Carlo (MC) and from the data. The background is described by empirical functions, as a Gaussian with a mass-dependent width or an exponential times a fourth-order polynomial. Finally the fit is performed in two invariant mass ranges ($2.2 < m_{\mu\mu} < 4.5$ GeV/c^2 and $2.0 < m_{\mu\mu} < 5.0$ GeV/c^2) for each combination of signal and background functions. In this procedure the $\psi(2S)$ mass and width are bound to the J/ψ ones according to the following relations: $m_{\psi(2S)} = m_{J/\psi} + (m_{J/\psi}^{\mathrm{PDG}} - m_{\psi(2S)}^{\mathrm{PDG}})$ and $\sigma_{\psi(2S)} = \sigma_{J/\psi} \cdot (\sigma_{\psi(2S)}^{\mathrm{MC}}/\sigma_{J/\psi}^{\mathrm{MC}})$, where $m_{J/\psi}$ and $\sigma_{J/\psi}$ are the mass and the width of J/ψ obtained from the fit of the invariant mass distribution, while m^{PDG} and σ^{MC} are the mass and widths of J/ψ and $\psi(2S)$ from PDG reference and Monte Carlo, respectively. The ratio $\sigma_{\psi(2S)}^{\mathrm{MC}}/\sigma_{J/\psi}^{\mathrm{MC}}$ has an uncertainty of 5% and it will be included as a systematic uncertainty on the $\psi(2S)$ yields. The final number of $\psi(2S)$ is obtained averaging the results of all the tests, the statistical uncertainty is the average of the statistical uncertainties of each test while the systematic one is the RMS of all the results. The results integrated over p_{T} and y are $N_{\psi(2S)}^{pPb} = 2929 \pm 231 \pm 216$ and $N_{\psi(2S)}^{Pbp} = 3348 \pm 278 \pm 348$ in p-Pb and Pb-p collisions respectively, where the first uncertainty is statistical and the second is the systematic one. In fig. 1 two examples of fits to the opposite sign invariant mass distributions are reported.

The acceptance times the efficiency $(A \times \epsilon)$ indicates the fraction of charmonia that can be reconstructed in the considered kinematic domain. $A \times \epsilon$ is evaluated with a Monte Carlo simulation. $\psi(2S)$ are generated according to p_{T} and y input distributions, which are tuned directly on data. The $A \times \epsilon$ p_{T}-integrated values are 0.2802 ± 0.0001 (p-Pb) and 0.2499 ± 0.0002 (Pb-p), where the uncertainty is statistical. A systematic uncertainty due to the choice of the input shapes is added and it ranges as a function of y from 2% to 5% in p-Pb and from 2% to 4% in Pb-p, and it is obtained adopting slightly different input shapes.
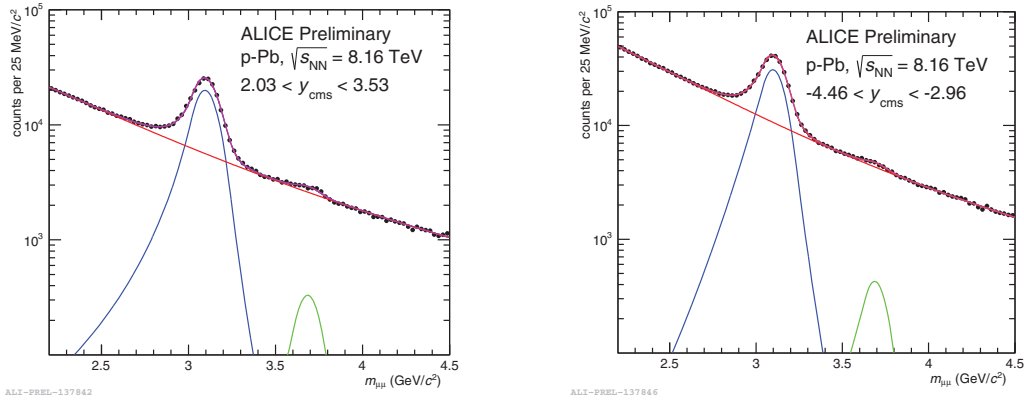
Fig. 1. – Fits to the opposite sign dimuon invariant mass distributions integrated over p_{T} in the range $2.03 < y_{\mathrm{cms}} < 3.53$ (left) and $-4.46 < y_{\mathrm{cms}} < -2.96$ (right). The J/ψ (blue curve) and $\psi(2S)$ (green curve) signal shapes are shown together with the background shape (red curve).

The formula used for the calculation of the nuclear modification factor is reported below:

$$(2) \qquad R_{\mathrm{pA}}^{\psi(2S)} = R_{\mathrm{pA}}^{J/\psi} \cdot \frac{\sigma_{pA}^{\psi(2S)}}{\sigma_{pA}^{J/\psi}} \cdot \frac{\sigma_{pp}^{J/\psi}}{\sigma_{pp}^{\psi(2S)}}$$

The $\psi(2S)$ R_{pA} can be evaluated starting from the J/ψ R_{pA} [3] multiplied by the $\psi(2S)/J/\psi$ cross section ratio in pA and pp collisions. $\sigma_{\mathrm{pp}}^{J/\psi}/\sigma_{\mathrm{pp}}^{\psi(2S)}$ is largely energy independent. Hence, in this analysis, the ratio evaluated at $\sqrt{s} = 7$ TeV is used [7], as it was already done for the evaluation of the $\psi(2S)$ R_{pA} in pA collisions at $\sqrt{s_{\mathrm{NN}}} = 5.02$ TeV [4]. This quantity has also an 8% uncertainty, which is the same for all the p_{T} and y bins and was meant to take into account residual effects related to the different centre of mass energy and the different rapidity range between the proton-proton and the proton-nucleus analysis.

In table I the sources of systematic uncertainties considered in the calculation of the nuclear modification factor and $\psi(2S)$ cross section are reported. Using the formula in eq. (2) some of the systematic uncertainties, like the systematic on trigger, tracking and matching, are common to the J/ψ and $\psi(2S)$ analysis by J/ψ and $\psi(2S)$, hence they cancel out. The main contribution to the systematic uncertainty on R_{pA} is given by the $\psi(2S)$ signal extraction and proton-proton reference.

4. – Results

The ratio between $\psi(2S)$ and J/ψ cross sections, named *single ratio*, represents a powerful tool to investigate nuclear effects on charmonium production. As mentioned before, one of the advantages of this ratio is the possibility that some of the systematic uncertainties in common between $\psi(2S)$ and J/ψ cancel out. In fig. 2 the single ratios at $\sqrt{s_{\mathrm{NN}}} = 5.02$ and 8.16 TeV are compared with ALICE results for p-Pb collisions. Results at $\sqrt{s_{\mathrm{NN}}} = 5.02$ and 8.16 TeV are compatible within 1σ, while comparing the results in

TABLE I. – *$\psi(2S)$ and J/ψ systematic uncertainties for both p-Pb and Pb-p. The first uncertainty refers to the value integrated over p_{T} and y, while the range in parenthesis corresponds to the maximum and minimum uncertainty both as a function of p_{T} and y.*

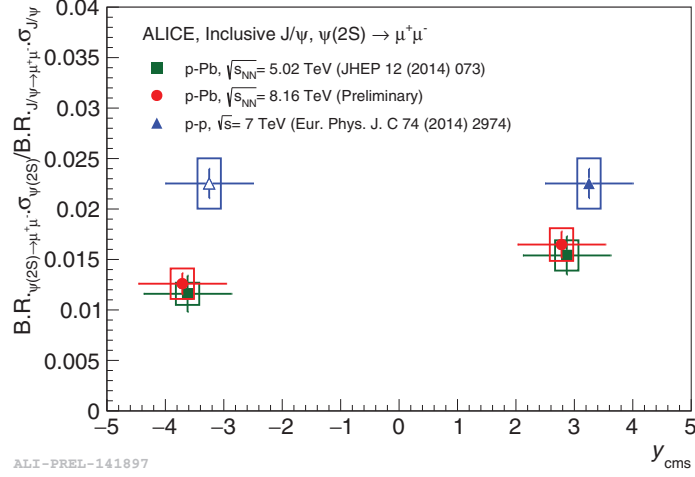|	$\psi(2S)$		J/ψ	
source	p-Pb (%)	Pb-p (%)	p-Pb (%)	Pb-p (%)
signal extraction	10 (9–20) + 5	6.4 (11–24) + 5	3 (2–3)	3 (2–3)
trigger	2.6	3.1	2.6	3.1
tracking	1	2	1	2
matching	1	1	1	1
MC inputs	3 (2–5)	1.5 (2–4)	0.5 (1–3)	0.5 (1–2)
pp reference	12 (12–17)	12 (12–17)	3 (2–6)	3 (2–7)

ALI-PREL-141897

Fig. 2. – $\sigma_{\psi(2S)}/\sigma_{J/\psi}$ single ratio integrated over p_{T} in p-Pb and Pb-p collisions at $\sqrt{s_{\mathrm{NN}}} = 5.02$ (green squares) and 8.16 TeV (red points). Results at $\sqrt{s_{\mathrm{NN}}} = 5.02$ TeV are slightly shifted in order to make them more visible. The ratio $\sigma_{\psi(2S)}/\sigma_{J/\psi}$ in pp collisions at $\sqrt{s} = 7$ TeV is also represented, the blue closed triangle refers to the measured quantity while the open one is obtained from the first by reflection around $y = 0$. The vertical bars represent the statistical uncertainties while the boxes correspond to the systematic ones (coloured version on-line).

proton-nucleus collisions with proton-proton ones at $\sqrt{s} = 7$ TeV a large discrepancy is visible, especially in the backward rapidity region.

Figure 3 shows the R_{pA} as a function of rapidity for $\psi(2S)$ and J/ψ. Since the nuclear modification factor is calculated as in eq. (2), this implies that some uncertainties are in common between the two sets of results. In this case the global error plotted as a light grey box around unity is the one on $R_{\mathrm{pA}}^{J/\psi}$, which is shared with the $\psi(2S)$ R_{pA} one and it amounts to $\sim 8\%$. The difference between the results for the two resonances is significant and it is larger than 1.5σ in the forward rapidity region, while in the backward one it is around 3σ. The values of the nuclear modification factor integrated over rapidity and
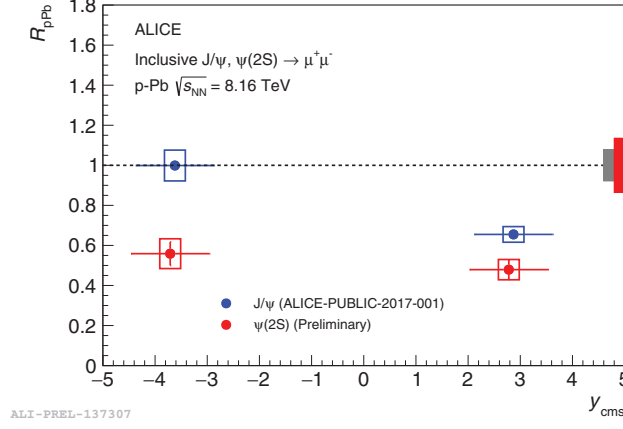
Fig. 3. – The $\psi(2S)$ nuclear modification factor compared to the same quantity for J/ψ as a function of y at $\sqrt{s_{\mathrm{NN}}} = 8.16\,\mathrm{TeV}$. The horizontal bars correspond to the width of the rapidity bins. The vertical bars represent the statistical uncertainties while the boxes corresponds to the systematic ones. The boxes around unity represent the global error on $\psi(2S)$ (red box) and the global error shared by $\psi(2S)$ and J/ψ (grey box) (coloured version on-line).

transverse momentum, separately in the backward and the forward rapidity regions are

$$R_{\mathrm{pA}}^{\psi(2S)}(2.03 < y_{\mathrm{cms}} < 3.53) = 0.48 \pm 0.05(stat) \pm 0.08(syst),$$

$$R_{\mathrm{pA}}^{\psi(2S)}(-4.46 < y_{\mathrm{cms}} < -2.96) = 0.56 \pm 0.06(stat) \pm 0.11(syst).$$

The sizeable $\psi(2S)$ statistics collected in proton-nucleus collisions allows for a differential study of the various observables as a function of p_{T} in five bins, from 0 to $12\,\mathrm{GeV}/c$. In fig. 4 the R_{pA} of $\psi(2S)$ and J/ψ as a function of p_{T} are shown in the forward and the backward rapidity regions. Given the smaller $\psi(2S)$ statistics with respect to the J/ψ one, a larger binning is used. As already observed in the results as a function of rapidity
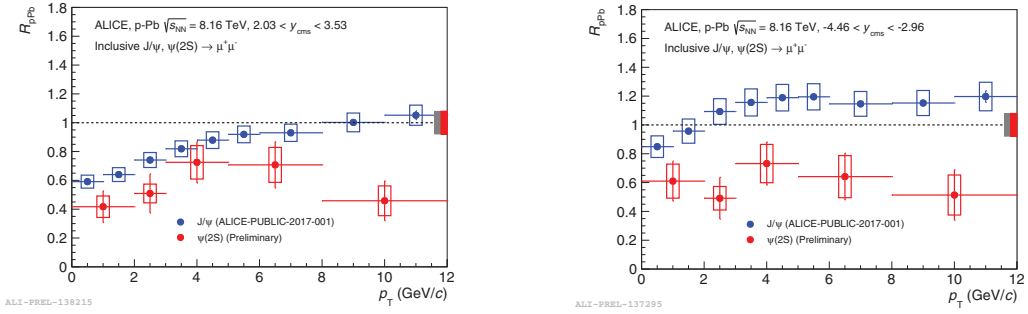

Fig. 4. – The nuclear modification factor for $\psi(2S)$ compared to the same quantity for J/ψ as a function of p_{T} for p-Pb (left) and Pb-p (right) collisions at $\sqrt{s_{\mathrm{NN}}} = 8.16\,\mathrm{TeV}$. The horizontal bars correspond to the width of the transverse momentum bins. The vertical bars represent the statistical uncertainties while the boxes correspond to the systematic uncertainties (coloured version on-line).
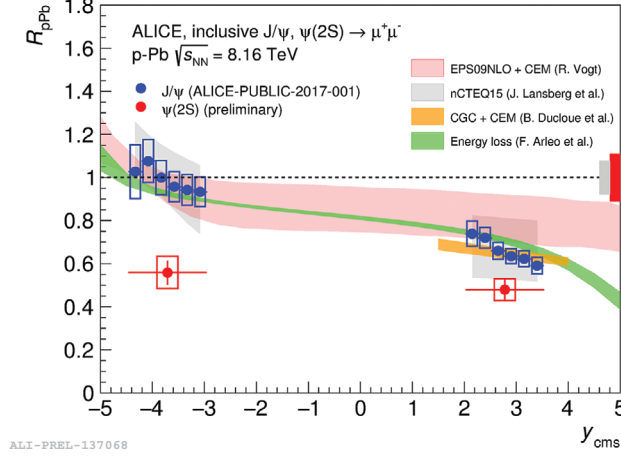
Fig. 5. – Nuclear modification factor of $\psi(2S)$ and J/ψ as a function of rapidity at $\sqrt{s_{\mathrm{NN}}} = 8.16$ TeV in proton-nucleus collisions. Results are compared with theoretical models which include only cold nuclear matter effects (coloured version on-line).

the nuclear modification factor points out to a more evident suppression for the $\psi(2S)$, especially in the range $-4.46 < y_{\mathrm{cms}} < -2.96$.

   $\psi(2S)$ and J/ψ are expected to be affected in a similar way by cold nuclear matter effects, in particular shadowing and energy loss, because there is no sensitivity of these processes to the final quantum numbers of the charmonium state produced. In fig. 5 the R_{pA} for the two resonances as a function of rapidity are compared with theoretical models which include only cold nuclear matter effects. While the R_{pA} of J/ψ is in good agreement with predictions, the $\psi(2S)$ shows a large deviation from theoretical models in particular in the backward rapidity region. The nuclear absorption of charmonium in the medium cannot explain this effect because it is relevant when the formation time (τ_f) of the resonance is smaller than the crossing time (τ_c) of the colliding particles, but
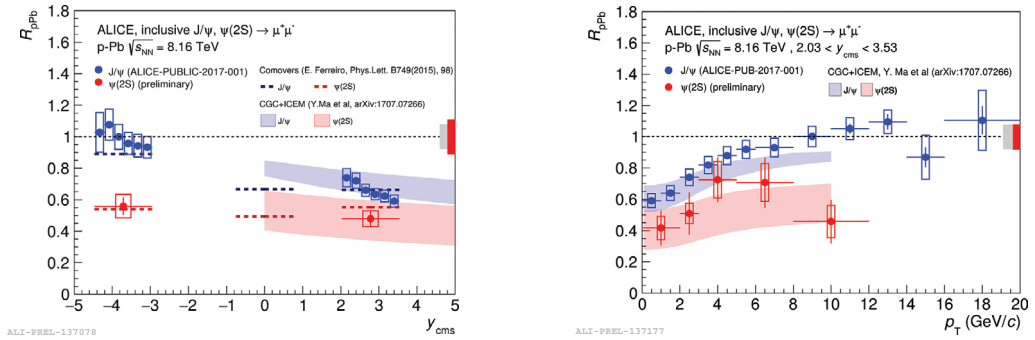

Fig. 6. – Nuclear modification factor of $\psi(2S)$ and J/ψ as a function of rapidity and transverse momentum at $\sqrt{s_{\mathrm{NN}}} = 8.16$ TeV at forward y in proton-nucleus collisions. Results are compared with theoretical predictions of the "comovers model" (dashed line) [10] and CGC+iCEM (coloured bands) [11] (coloured version on-line).

at $\sqrt{s_{NN}} = 8.16$ TeV $\tau_f \sim \tau_c$. The anomalous suppression of the $\psi(2S)$ can be explained comparing data with models which include the interaction of the $c\bar{c}$ states with *comovers*. In general this term indicates particles produced in the collision which move with the $c\bar{c}$ pair and can dissociate it producing the suppression effect observed for $\psi(2S)$, because of its lower binding energy with respect to the J/ψ. In fig. 6 the R_{pA} of $\psi(2S)$ and J/ψ is compared with two theoretical models which include the interaction with comoving particles and the agreement is good for the R_{pA} as a function of p_T and y. In details:

- the "comovers model" [10] includes the interaction of the nascent charmonium resonance with soft particles produced in the collision and since their formation time is boosted by Lorentz dilation they can continue to interact even outside the nuclear volume.

- in the "CGC+iCEM" model [11] the production of the $c\bar{c}$ pairs is described considering the *colour glass condensate* (CGC) and the hadronization process is the *improved colour evaporation model*. In this model the interaction between comovers and $c\bar{c}$ pairs is already introduced at a partonic level.

5. – Conclusion

In this paper the $\psi(2S)$ production in proton-nucleus collisions at $\sqrt{s_{NN}} = 8.16$ TeV, in two rapidity ranges, $2.03 < y_{cms} < 3.53$ and $-4.46 < y_{cms} < -2.96$, has been presented. The statistics collected is larger than in the $\psi(2S)$ analysis at $\sqrt{s_{NN}} = 5.02$ TeV [4], allowing an improved precision of the measurements. Results have been evaluated in terms of single ratio $(\sigma_{\psi(2S)}/\sigma_{J/\psi})_{pA}$ and nuclear modification factor R_{pA} and these quantities have been studied as a function of p_T and y. Finally the R_{pA} is compared with various theoretical models. In general it has been observed that:

- $\psi(2S)$ shows a large suppression at both forward and backward rapidity;

- the comparison between $\psi(2S)$ results at $\sqrt{s_{NN}} = 5.02$ and 8.16 TeV indicates a similar suppression in the forward and in the backward rapidity region at both energies;

- $\psi(2S)$ is more suppressed than J/ψ, especially at backward rapidity where the effect is around 3σ.

The nuclear modification factor of $\psi(2S)$ and J/ψ at $\sqrt{s_{NN}} = 8.16$ TeV has been compared with theoretical predictions including only cold nuclear matter effects (CNM). The stronger $\psi(2S)$ suppression observed cannot be explained only by cold nuclear matter effects and supports the presence of additional mechanisms. Results are then compared with other models including final state effects as the interaction with *comoving* particles (hadrons or partons). In this case the predictions are in good agreement with experimental results. Therefore, the results presented in this paper give an interesting indication for the production of a dense system not only in Pb-Pb collisions but also in p-Pb. Although the precise nature of this system (a dense hadronic gas or a QGP droplet) is still under debate, these results provide an intriguing indication for an *a priori* unexpected effect that surely deserves further studies.

REFERENCES

[1] MATSUI T. and SATZ H., *Phys. Lett. B*, **178** (1986) 416.
[2] ARLEO F., KOLEVATOV R., PEIGN S. and RUSTAMOVA M., *JHEP*, **05** (2013) 155.
[3] ALICE COLLABORATION, *Preliminary Physics Summary: Inclusive J/ψ production at forward rapidity in p-Pb collisions at* $\sqrt{s_{\mathrm{NN}}} = 8.16$ *TeV*, ALICE-PUBLIC-2017-001.
[4] ALICE COLLABORATION (ABELEV B. B. *et al.*), *JHEP*, **12** (2014) 073.
[5] ALICE COLLABORATION (AAMODT K. *et al.*), *JINST*, **3** (2008) S08002.
[6] ALICE COLLABORATION (ABELEV B. B. *et al.*), *Int. J. Mod. Phys. A*, **29** (2014) 1430044.
[7] ALICE COLLABORATION (AAMODT K. *et al.*), *Phys. Lett. B*, **704** (2011) 442; **718** (2012) 692(E).
[8] PARTICLE DATA GROUP (OLIVE K. A. *et al.*), *Chin. Phys. C*, **38** (2014) 090001.
[9] ALICE COLLABORATION, *Quarkonium signal extraction in ALICE*, ALICE-PUBLIC-2015-006.
[10] FERREIRO E. G., *Phys. Lett. B*, **749** (2015) 98.
[11] MA Y. Q., VENUGOPALAN R., WATANABE K. and ZHANG H. F., *ψ(2S)/J/ψ suppression in proton-nucleus collisions from factorization violating soft color exchanges*, arXiv:1707.07266 [hep-ph].